Inorganic Chemistry
Cite This: Inorg. Chem. XXXX, XXX, XXX–XXX
Article
pubs.acs.org/IC

Hydrogen-Bonding Effects in Five-Coordinate High-Spin Imidazole-Ligated Iron(II) Porphyrinates

Chuanjiang Hu,*[,†,‡] Bruce C. Noll,[‡] Charles E. Schulz,[§] and W. Robert Scheidt*[,‡]

[†]Contribution from State and Local Joint Engineering Laboratory for Novel Functional Polymeric Materials, College of Chemistry, Chemical Engineering and Materials Science, Soochow University, Suzhou 215123, Jiangsu, People's Republic of China

[‡]The Department of Chemistry and Biochemistry, University of Notre Dame, Notre Dame, Indiana 46556, United States

[§]Department of Physics, Knox College, Galesburg, Illinois 61401, United States

Supporting Information

ABSTRACT: The influence of hydrogen binding to the N−H group of coordinated imidazole in high-spin iron(II) porphyrinates has been studied. The preparation and characterization of new complexes based on [Fe(TPP)(2-MeHIm)] (TPP is the dianion of tetraphenylporphyrin) are reported. The hydrogen bond acceptors are ethanol, tetramethylene sulfoxide, and 2-methylimidazole. The last acceptor, 2-MeHIm, was found in a crystalline complex with two [Fe(TPP)(2-MeHIm)] sites, only one of which has the 2-methylimidazole hydrogen bond acceptor. This latter complex has been studied by temperature-dependent Mössbauer spectroscopy. All new complexes have also been characterized by X-ray structure determinations. The Fe−N_P and Fe−N_{Im} bond lengths, and displacement of the Fe atom out of the porphyrin plane are similar to, but marginally different than, those in imidazole-ligated species with no hydrogen bond. All the structural and Mössbauer properties suggest that these new hydrogen-bonded species have the same electronic configuration as imidazole-ligated species with no hydrogen bond. These new studies continue to show that the effects of hydrogen bonding in five-coordinate high-spin iron(II) systems are subtle and challenging to understand.

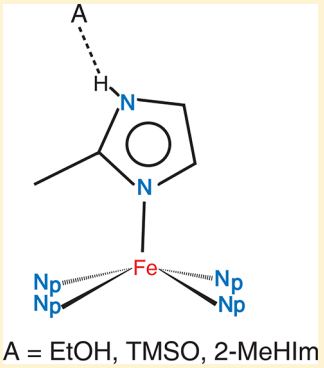

INTRODUCTION

Understanding the importance of secondary coordination sphere effects on the properties of biological coordination complexes in proteins, including hemes, has attracted considerable recent attention.[1,2] Possible second coordination sphere interactions include electrostatic interactions, π-stacking, steric interactions, and hydrogen bonding. Of these, hydrogen bonding effects are the most prevalent.[3−7] In heme proteins, the ligand binding pocket environment provides hydrogen bonds to the coordinated axial ligand through the protein side chains and can provide a wide range of hydrogen bond strengths thought to modulate protein function.[8−17]

Heme proteins with histidine as the fifth ligand range from (a) the O_2-carrying/storing proteins with weak hydrogen bonds from a nearby protein carbonyl to (b) peroxidases with medium to strong hydrogen bonds to conserved aspartates to (c) oxidases with medium to strong hydrogen bonds to conserved glutamates. Coordinated imidazolate has been taken as the limit of a strong hydrogen bond. The differences between coordinated imidazole and coordinated imidazolate are quite profound but readily studied in small molecule systems. Although imidazole- and imidazolate-ligated iron(II) porphyrinates both exhibit an $S = 2$ (quintet) state, the structural parameters of the coordination groups are distinct with both axial and equatorial bond distance differences and large differences in the displacement of iron from the porphyrin plane.[18] Distinctive features in the Mössbauer spectra are seen in both zero field and applied magnetic fields. Spectra in applied magnetic fields show that the doubly occupied d-orbital is different in imidazole- vs imidazolate-ligated iron(II) porphyrinates. The positive sign of the quadrupole splitting in the imidazolate derivative indicates that the doubly occupied orbital must be the d_{xy}-orbital, whereas the negative sign in the imidazole derivative is consistent only with a low-symmetry orbital comprised of a hybrid of d_{xz} and an unoccupied porphyrin E(g) orbital. This change in the d-electron configuration is clearly consistent with all observed differing features of the two classes.[19,20] Where do hydrogen-bonded imidazoles fit into this divide?

Directly studying how hydrogen bonding affects the electronic structure and other properties of imidazole-ligated high-spin iron(II) has proven to be quite challenging. The requirements for adequate systems with imidazole-ligated N−H hydrogen bonds are substantial. First, isolation of a well-characterized solid-state material is a must. Obtaining five-coordinate high-spin imidazole-ligated species requires sterically hindered imidazoles (at the 2-position) to prevent coordination of a second imidazole and thus stop formation of a six-coordinate low-spin species.[21] The imidazole must also have an N−H group to interact with an added hydrogen-bond acceptor. A possible complication is that the hydrogen bond

Received: October 26, 2017

DOI: 10.1021/acs.inorgchem.7b02744
Inorg. Chem. XXXX, XXX, XXX–XXX

Table 1. Brief Crystallographic Data and Data Collection Parameters

	[Fe(TPP)(2-MeHIm)]·(TMSO)	[Fe(TPP)(2-MeHIm)]·0.5(C_6H_5Cl)	[Fe(TPP)(2-MeHIm)]·(C_2H_5OH)	2[Fe(TPP)(2-MeHIm)]·(2-MeHim)·(C_6H_5Cl)
formula	$C_{48}H_{34}FeN_6$·(C_4H_8OS)	$C_{48}H_{34}FeN_6$·0.5(C_6H_5Cl)	$C_{48}H_{34}FeN_6$·(C_2H_5OH)	2($C_{48}H_{34}FeN_6$)·C_6H_5Cl·$C_4H_6N_2$
formula weight, FW	854.82	806.93	796.73	1695.98
a, Å	17.660(8)	17.904(4)	17.0715(6)	13.1422(3)
b, Å	16.193(7)	10.151(2)	16.0697(6)	16.8224(4)
c, Å	14.670(4)	23.061(5)	14.6295(5)	20.0115(5)
α, deg	90	90	90	75.147(1)
β, deg	99.07(2)	108.47(3)	98.702(3)	80.413(1)
γ, deg	90	90	90	89.629(1)
V, Å^3	4143(3)	3975.2(15)	3967.2(2)	4213.61(18)
Z	4	4	4	2
space group	*C*2/*c*	$P2_1/n$	*C*2/*c*	$P\bar{1}$
D_c, g/cm^3	1.370	1.348	1.334	1.337
F(000)	1784	1676	1664	1764
μ, mm^{-1}	0.463	0.458	0.428	0.437
crystal dimens, mm	0.46 × 0.12 × 0.12	0.52 × 0.27 × 0.14	0.43 × 0.08 × 0.07	0.32 × 0.31 × 0.29
absorption correction	SADABS			
radiation, Mo K*α*, $\bar{\lambda}$	0.71073 Å			
T, K	100(2)	100(2)	100(2)	100(2)
total data collected	33 866	61 219	35 328	128 313
unique data	4927 (R_{int} = 0.044)	14460 (R_{int} = 0.030)	4168 (R_{int} = 0.034)	23284 (R_{int} = 0.032)
unique obsd data[I > 2 *σ*(I)]	4188	12 089	3852	18 785
refinement method	on F^2 (SHELXL)			
final *R* indices [I > 2*σ*(I)]	R_1 = 0.0433, wR_2 = 0.1094	R_1 = 0.0398, wR_2 = 0.1025	R_1 = 0.0312, wR_2 = 0.0750	R_1 = 0.0583, wR_2 = 0.1497
final *R* indices [for all data]	R_1 = 0.0542, wR_2 = 0.1146	R_1 = 0.0510, wR_2 = 0.1127	R_1 = 0.0403, wR_2 = 0.0814	R_1 = 0.0731, wR_2 = 0.1601

DOI: 10.1021/acs.inorgchem.7b02744
Inorg. Chem. XXXX, XXX, XXX−XXX

acceptor can lead to displacement of the original imidazole ligand.

An important result, which demonstrated how significant hydrogen bonding can be, was found in an unusual crystalline system that had two independent [Fe(TPP)(2-MeHIm)] molecules.[22,23] One molecule had an external 2-MeHIm as the hydrogen bond acceptor; the other site had no hydrogen bond to the coordinated imidazole. The system was characterized by both X-ray and neutron diffraction structure determinations and Mössbauer measurements in both zero and applied magnetic field. There were clear differences between the sites. Both the structural details and the Mössbauer results suggest that one site has imidazolate-like character and the other site is comparable to other imidazole derivatives. Attempts to replicate this strong hydrogen bonding via the addition of several hindered pyridines as the hydrogen bond acceptors either failed or, surprisingly, gave the same two-site system.[23,24]

A later attempt to study hydrogen-bonding effects made use of 1,10-phenanthroline as the acceptor in five-coordinate high-spin iron(II).[25] This use of 1,10-phenanthroline followed earlier results that demonstrated enhanced imidazole binding contributions in six-coordinate iron(III) complexes.[26,27] The consequences of the relatively weak hydrogen bonds formed between coordinated imidazole and 1,10-phenanthroline were found to have a small or no effect on the electronic structure of the high-spin iron(II) species in either of the two species characterized.

In this paper, we report on new attempts to obtain crystalline materials with hydrogen bonding acceptors. This investigation provides further examples with hydrogen-bonded, coordinated imidazole with three examples described. All of the new examples show that hydrogen bonding has only small effects on either the electronic or molecular structures. Most surprising was the isolation of a new two-site system with a hydrogen-bonded imidazole site and a second site with no hydrogen bond. Although there are many similarities between this two-site system and an earlier system,[23] the major effects of hydrogen bonding observed in the first system are not found. The new studies continue to show that the effects of hydrogen bonding in five-coordinate high-spin iron(II) systems are subtle and challenging to understand.

EXPERIMENTAL SECTION

General Information. All reactions and manipulations for the preparation of the iron(II) porphyrin derivatives (see below) were carried out under argon, using a double-manifold vacuum line, Schlenkware, and cannula techniques. Chlorobenzene was washed with concentrated sulfuric acid, then with water until the aqueous layer was neutral, dried with $MgSO_4$, and distilled twice over P_2O_5 under argon. Hexanes were distilled over sodium benzophenone. 2-Methylimidazole (Aldrich) was recrystallized from toluene/methanol and dried under vacuum. All other chemicals were used as received from Aldrich or Fisher Scientific. The free-base porphyrin *meso*-tetraphenylporphyrin (H_2TPP) was prepared according to Adler et al.[28] The metalation of the free-base porphyrin to give [Fe(TPP)Cl] was done as previously described.[29] $[Fe(TPP)]_2O$ was prepared according to a modified Fleischer preparation.[30] The ^{57}Fe-enriched porphyrinate was prepared using a modified small-scale metalation procedure described by Landergren and Baltzer.[31] The $^{57}Fe_2O_3$ used in the ^{57}Fe labeled complex was purchased from Cambridge Isotopes.

Mössbauer measurements were performed on a constant acceleration spectrometer from 25 K to 250 K with optional small field (Knox College) that was equipped with a Joule−Thompson refrigerator for temperature control. For [Fe(TPP)(2-MeHIm)]·(2-MeHIm)·(C_6H_5Cl), an ^{57}Fe sample was prepared for Mössbauer spectroscopy, and the unit cell of the crystals used were checked before the Mössbauer measurements. The crushed crystalline sample then was immobilized in Apiezon M grease mull.

Synthesis of 2[Fe(TPP)(2-MeHIm)]·(2-MeHIm)·(C_6H_5Cl). $[Fe(TPP)]_2O$ (32 mg, 0.024 mmol) was mixed with ethanethiol (1 mL) in chlorobenzene (8 mL) and stirred for 3 days at room temperature. The resulting solution of four-coordinate [Fe(TPP)] was transferred into a Schlenk flask containing 2-methylimidazole (17 mg, 0.21 mmol) and 2,4,6-collidine (0.25 mL, 1.9 mmol). The mixture was stirred for 1 h. X-ray-quality crystals were obtained in 8 mm × 250 mm sealed glass tubes by liquid diffusion using hexanes as nonsolvent after five months.

Synthesis of [Fe(TPP)(2-MeHIm)]·0.5(C_6H_5Cl). $[Fe(TPP)]_2O$ (38 mg, 0.029 mmol) was mixed with ethanethiol (1 mL) in chlorobenzene (8 mL), and stirred for 3 days at room temperature. The resulting solution of four-coordinate [Fe(TPP)] was transferred into a Schlenk flask containing 2-methylimidazole (75 mg, 0.93 mmol) and 2,4,6-collidine (0.25 mL, 1.9 mmol). The mixture was stirred for 1 h. X-ray-quality crystals were obtained in 8 mm × 250 mm sealed glass tubes by liquid diffusion using hexanes as nonsolvent after one month.

Synthesis of [Fe(TPP)(2-MeHIm)]·(C_2H_5OH). $[Fe(TPP)]_2O$ (76 mg, 0.058 mmol) was mixed with ethanethiol (1.5 mL) in chlorobenzene (12 mL), and stirred for 3 days at room temperature. The resulting solution of four-coordinate [Fe(TPP)] was transferred into a Schlenk flask containing 2-methylimidazole (36 mg, 0.44 mmol). The mixture was stirred for 1 h. The resulting solution was transferred into 8 mm × 250 mm sealed glass tubes and layered with a 2-methylimidazole solution (0.12 mol/L) in ethanol. X-ray-quality crystals were obtained after 2 weeks.

Synthesis of [Fe(TPP)(2-MeHIm)]·TMSO. $[Fe(TPP)]_2O$ (31 mg, 0.023 mmol) was mixed with ethanethiol (0.6 mL) in chlorobenzene (6 mL), and stirred for 3 days at room temperature. The resulting solution of four-coordinate [Fe(TPP)] was transferred into a Schlenk flask containing 2-methylimidazole (11 mg, 0.13 mmol) and tetramethylene sulfoxide (TMSO, 0.5 mL, 5.8 mmol). The mixture was stirred for 1 h. X-ray-quality crystals were obtained in 8 mm × 250 mm sealed glass tubes by liquid diffusion using hexanes as nonsolvent after 2 weeks.

X-ray Structure Determinations. Single-crystal experiments were carried out on a Bruker Apex system with graphite-monochromated Mo Kα radiation (λ = 0.71073 Å). All structures were solved by direct methods and refined against F^2 using SHELXTL;[32,33] subsequent difference Fourier syntheses led to the location of most of the remaining non-hydrogen atoms. All nonhydrogen atoms were refined anisotropically if not remarked otherwise below. Hydrogen atoms were added with the standard SHELXL idealization methods. The program SADABS[34] was applied for the absorption correction. Brief crystal data and intensity collection parameters for the crystalline complexes are shown in Table 1. Complete crystallographic details, atomic coordinates, anisotropic thermal parameters, and fixed hydrogen atom coordinates are given in the Supporting Information.

[Fe(TPP)(2-MeHIm)]·0.5(C_6H_5Cl). A red crystal with dimensions of 0.14 mm × 0.27 mm × 0.52 mm was used for the structure determination. Crystal data were collected at 100 K. The structure was refined in space group $P2_1/n$ with no restraints applied. The asymmetric unit contains one porphyrinate molecule and half a chlorobenzene solvate molecule. The 2-methylimidazole molecule was found to be disordered over two positions. After the final refinement, the occupancy of the major orientation was found to be 81%. The two imidazole rings are essentially coplanar; the dihedral angle is ~2.5°. The chlorobenzene solvate is disordered around inversion centers.

[Fe(TPP)(2-MeHIm)]·(C_2H_5OH). A red crystal with the dimensions 0.43 mm × 0.08 mm × 0.07 mm was used for the structure determination. Crystal data were collected at 100 K. The structure was refined in space group $C2/c$ with no restraints applied. The molecule has required 2-fold symmetry and thus the asymmetric unit contains a half porphyrinate molecule and a half ethanol solvate.

DOI: 10.1021/acs.inorgchem.7b02744
Inorg. Chem. XXXX, XXX, XXX−XXX

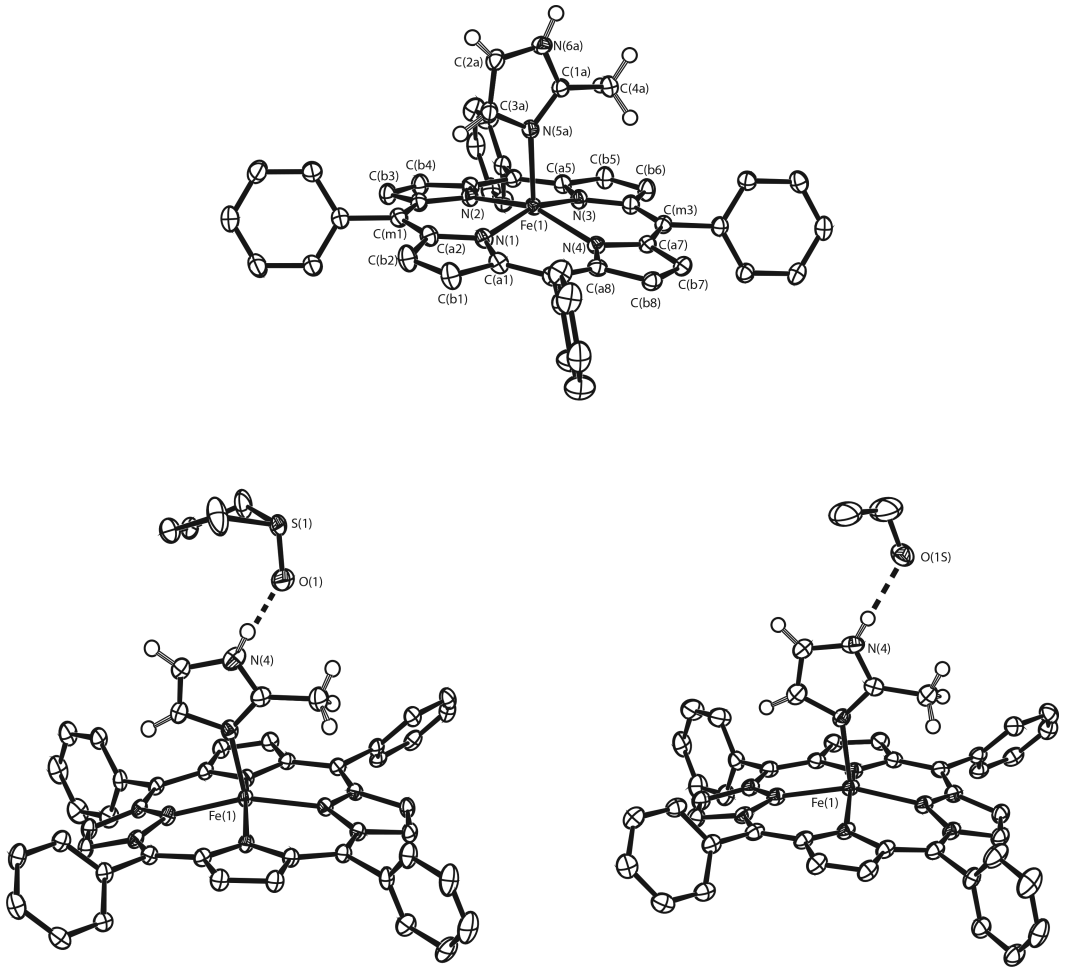

Figure 1. ORTEP diagrams of three [Fe(TPP)(2-MeHIm)] molecules, all ellipsoids are contoured at the 50% probability level. For clarity, only one orientation of the disordered imidazole ring and only the imidazole hydrogen N−H and methyl group hydrogen atoms are shown. The top diagram is the [Fe(TPP)(2-MeHIm)]·0.5(C_6H_5Cl) solvate. The bottom left diagram is that for the [Fe(TPP)(2-MeHIm)]·(TMSO) solvate; the N···O hydrogen bond distance is 2.744 Å. The bottom right diagram is that for the [Fe(TPP)(2-MeHIm)]·(EtOH) solvate; the N···O hydrogen bond distance is 2.880 Å.

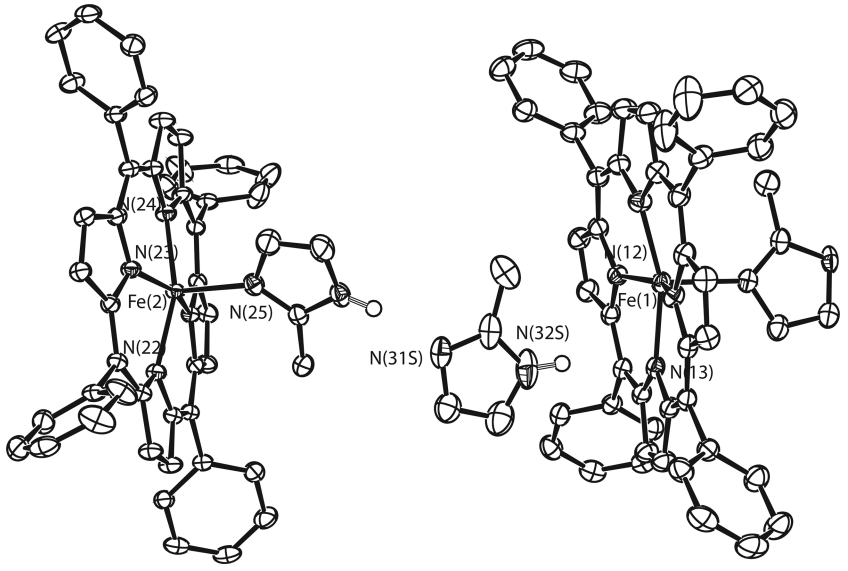

Figure 2. ORTEP diagram of the two [Fe(TPP)(2-MeHIm)] molecules in the two site system. Molecule **1′** is shown on the right (the coordinated imidazole is disordered, with a major occupancy of 0.642). Molecule **2′** is shown on the left, with a completely ordered imidazole. The hydrogen bond formed with the imidazole solvate has a N···N distance of 2.843 Å.

DOI: 10.1021/acs.inorgchem.7b02744
Inorg. Chem. XXXX, XXX, XXX−XXX

[Fe(TPP)(2-MeHIm)]·TMSO. A red crystal with the dimensions 0.12 mm × 0.12 mm × 0.46 mm was used for the structure determination. Crystal data were collected at 100 K. The structure was refined in space group $C2/c$. The molecule has required 2-fold symmetry and, thus, the asymmetric unit contains half a porphyrinate molecule and half a tetramethylene sulfoxide solvate molecule.

2[Fe(TPP)(2-MeHIm)]·(2-MeHim)·(C_6H_5Cl). A red crystal with the dimensions 0.29 mm × 0.31 mm × 0.32 mm was used for the structure determination. Crystal data were collected at 100 K. The structure was refined in space group $P\bar{1}$ with no restraints applied. The asymmetric unit contains two independent five-coordinate [Fe(TPP)(2-MeHIm)] molecules, one chlorobenzene molecule, and one 2-methylimidazole molecule of solvation. The imidazole ligand associated with molecule one is disordered with occupancies of 0.64 and 0.36. The two imidazole rings are essentially coplanar; the dihedral angle is ∼2.2°. One phenyl ring of molecule one is disordered with occupancies of 0.70 and 0.30. The chlorobenzene solvate is also disordered with final refined occupancies of 0.75 and 0.25. The second molecule is completely ordered.

RESULTS

The molecular structure of four iron(II) tetraphenylporphyrinates coordinated by the sterically hindered 2-methylimidazole ligand are reported. The use of 2-methylimidazole ensures that a high-spin five-coordinate complex results. Three crystalline derivatives, illustrated in Figure 1, provide a structure for a single [Fe(TPP)(2-MeHIm)] molecule. Two derivatives have a hydrogen-bonded solvate molecule that are shown in the diagrams. ORTEP diagrams with all atoms labeled are given in the Supporting Information.

Figure 2 displays the ORTEP diagram of an interesting system containing two [Fe(TPP)(2-MeHIm)] molecules along with a third 2-methylimidazole and a chlorobenzene molecule as molecules of solvation in the asymmetric unit of structure. ORTEP diagrams with all atoms labeled are given in the Supporting Information. There are thought-provoking similarities and differences with another system that has two [Fe(TPP)(2-MeHIm)] molecules along with a 2-methylimidazole solvate in the asymmetric unit.[23] These differences and similarities will be discussed in detail in the Discussion section.

Variable-temperature Mössbauer spectra were obtained on this two-site system. To ensure that the exact same phase as the X-ray crystalline sample was measured by Mössbauer, an ^{57}Fe labeled sample was prepared and crystallized. Cell constants were determined on several ^{57}Fe sample crystals. These crystals were then crushed, immobilized, and measured. Table 2 reports the measurements taken from 25 K to 298 K.

Table 2. Variable-Temperature Mössbauer Parameters for 2[Fe(TPP)(2-MeHIm)]·(2-MeHIm)·(C_6H_5Cl)]

			Line Width, Γ (mm/s)	
temperature, T (K)	ΔE_Q (mm/s)	δ_{Fe} (mm/s)	left	right
295	1.818	0.796	0.276	0.273
250	1.873	0.832	0.307	0.303
200	1.985	0.862	0.325	0.322
150	2.053	0.876	0.341	0.327
100	2.171	0.887	0.328	0.316
50	2.254	0.897	0.322	0.323
25	2.266	0.900	0.210	0.205

DISCUSSION

We have been investigating the effects of deprotonation of and/or hydrogen bonding to the N−H group of a coordinated imidazole in five-coordinate high-spin iron(II) porphyrinates. The effects of deprotonation of the imidazole are quite clear and lead to substantial changes in both the coordination group geometry[18,35] and the electronic structure of the high-spin Fe center, including a change in sign of the Mössbauer splitting.[18,20,35] The sign of the quadrupole splitting of imidazole derivatives are negative, whereas that of imidazolate derivatives are positive; this is the important consequence of differing populations of the $3d^6$ electron manifold in these high-spin complexes with a neutral vs an anionic axial ligand.[20,35]

The effects of hydrogen bonding to the imidazole are less clear-cut. It might be expected that a strong hydrogen bond to the imidazole would lead to imidazolate character for the ligand and thus lead to changes for the overall complex as well. This appeared to be the case in an earlier study, that of a two-site system: one site with an imidazole solvate molecule strongly hydrogen bonded to the imidazole of [Fe(TPP)(2-MeHIm)] and the second site with no hydrogen bond. Investigation showed that the first site had structural properties tending toward that of imidazolate systems, whereas the second site had geometric parameters typical of "normal" imidazole derivatives.[23] The Mössbauer spectra of this two-site system showed two distinct quadrupole doublets, with one quadrupole doublet at least partially similar to the imidazolate systems, although the sign of the quadrupole splittings could not be made with complete confidence.[23] However, a later study in which the coordinated imidazole was hydrogen-bonded to the N atoms of 1,10-phenanthroline displayed much smaller geometric effects and with the sign of the Mössbauer quadrupole splitting the same as that of imidazole systems with no hydrogen bonding.[25]

We hoped to clarify our understanding of these systems and have now prepared additional five-coordinate high-spin iron(II) species with a hydrogen-bonded imidazole. In this paper, we report on four systems, three of which satisfy the condition of an imidazole hydrogen-bonded to an external acceptor. The results of these new studies show that the effects of hydrogen bonding are subtle and challenging to understand.

All systems begin with the [Fe(TPP)(2-MeHIm)] base complex. Two derivatives have either tetramethylene sulfoxide or ethanol as the hydrogen bond acceptor. The ethanol derivative has been reported previously,[36,37] but complete structural details were never published. The third derivative is a two-site system with one [Fe(TPP)(2-MeHIm)] molecule hydrogen-bonded to a 2-methylimidazole solvate molecule, and the other [Fe(TPP)(2-MeHIm)] molecule is not hydrogen-bonded. This system has some formal similarity to a previously reported system,[23] but significant differences are found. The final derivative is a chlorobenzene solvate with no hydrogen bond present.

We first consider structural aspects of these five-coordinate high-spin iron(II) systems. The first structure of this type was [Fe(TPP)(2-MeHIm)]·(C_2H_5OH)[36,37] that revealed an interesting and unusual structural feature, that of a substantial doming of the porphyrin core. This doming can be specified by the difference in the displacement of the iron(II) from the mean plane of the four N atoms (ΔN_4) from the mean plane of the 24-atom core (Δ). The Fe atom displacement values for

DOI: 10.1021/acs.inorgchem.7b02744
Inorg. Chem. XXXX, XXX, XXX−XXX

Table 3. Selected Bond Distances and Angles for New Structures and Related Species[a]

	Bond Distances (Å)					Bond Angles (deg)				
complex[b]	Fe−N$_p$[c]	Fe−N$_{im}$	ΔN$_4$[d]	Δ[e]	Ct···N	Fe−N−C[f]	Fe−N−C[g]	θ[h]	ϕ[i]	ref
[Fe(TPP)(2-MeHIm)]·(1,10-phen) (**A**)	2.084(5)	2.1289(13)	0.38	0.47	2.049	132.03(12)	123.09(11)	8.8	18.5	25
[Fe(TPP)(2-MeHIm)]·(1,10-phen) (**B**)	2.080(9)	2.125(3)	0.36	0.39	2.049	130.8(2)	123.8(2)	6.6	17.7	25
	2.081(6)	2.120(3)	0.36	0.38	2.051	133.7(2)	121.5(2)	5.4	7.8	25
[Fe(OEP)(2-MeHIm)]·(1,10-phen)	2.088(14)	2.135(2)	0.39	0.49	2.051	132.75(17)	121.20(16)	2.7	8.1	25
	2.087(14)	2.131(2)	0.39	0.47	2.051	133.43(17)	121.66(17)	2.1	13.8	25
[Fe(TPP)(2-MeHIm)]·(C_2H_5OH)	2.086(8)	2.161(5)	0.42	0.55	2.044	131.4(4)	122.6(4)	10.3	6.5	36
[Fe(TPP)(2-MeHIm)]·(C_2H_5OH)	2.087(12)	2.144(1)	0.40	0.55	2.048	130.84(9)	123.32(9)	7.9	6.9	this work
[Fe(TPP)(2-MeHIm)]·(TMSO)	2.089(3)	2.142(2)	0.40	0.54	2.050	131.48(13)	122.84	8.0	3.6	this work
average of the eight values	2.084(4)	2.136(13)	0.39(2)	0.48(7)	2.049(2)	130.1(11)	122.5(9)	6.5(28)	10.(6)	
[Fe(OEP)(1,2-Me_2Im)]	2.080(6)	2.171(3)	0.37	0.45	2.047	132.7(3)	121.4(2)	3.8	10.5	19
[Fe(OEP)(2-MeHIm)]	2.077(7)	2.135(3)	0.34	0.46	2.049	131.3(3)	122.4(3)	6.9	19.5	19
[Fe(TPP)(1,2-Me_2Im)]	2.079(8)	2.158(2)[j]	0.36	0.42	2.048	129.3(2)	124.9(2)	11.4	20.9	38
[Fe(TTP)(2-MeHIm)]	2.076(3)	2.144(1)	0.32	0.39	2.050	132.8(1)	121.4(1)	6.6	35.8	38
[Fe(T*p*-OCH_3PP)(2-MeHIm)]	2.087(7)	2.155(2)[j]	0.39	0.51	2.049	130.4(2)	123.4(2)	8.6	44.5	38
[Fe(T*p*-OCH_3PP)(1,2-Me_2Im)]	2.077(6)	2.137(4)	0.35	0.38	2.046	131.9(3)	122.7(3)	6.1	20.7	38
[Fe(TPP)(2-MeHIm)]·1.5(C_6H_5Cl)	2.073(9)	2.127(3)[j]	0.32	0.38	2.049	131.1(2)	122.9(2)	8.3	24.0	39
[Fe(TPP)(2-MeHIm)]·0.5(C_6H_5Cl)	2.084(11)	2.1569(12)[j]	0.36	0.48	2.053	130.67(9)	123.07(10)	7.8	21.8	this work
average of the eight values	2.079(5)	2.148(15)	0.35(2)	0.43(5)	2.049(2)	131.3(12)	122.8(11)	7.4(22)	25.(10)	
[Fe(TPP)(2-MeHIm)] (Mol **1**)	2.080(8)	2.120(2)	0.36	0.41	2.050	131.6(1)	122.4(1)	9.2	16.0	23
[Fe(TPP)(2-MeHIm)]·(2-MeHIm) (Mol **2**)	2.099(7)	2.099(2)	0.49	0.55	2.040	129.0(1)	125.7(1)	7.6	22.9	23
[Fe(TPP)(2-MeHIm)] (Mol **1′**)	2.084(9)	2.164(2)[j]	0.39	0.42	2.051	132.3(2)	122.4(1)	7.9	12.4	this work
[Fe(TPP)(2-MeHIm)]·(2-MeHIm) (Mol **2′**)	2.083(9)	2.125(2)	0.38	0.44	2.050	132.0(2)	122.9(2)	4.1	40.5	this work
[K(222)][Fe(OEP)(2-MeIm$^-$)]	2.113(4)	2.060(2)	0.56	0.65	2.036	136.6(2)	120.0(2)	3.6	37.4	18
[K(222)][Fe(TPP)(2-MeIm$^-$)]	2.118(13)	1.999(5)	0.56	0.66	2.044	129.6(3)	126.7(3)	9.8	23.4	18
		2.114(5)				133.6(4)	121.9(4)	6.5	21.6	
[Fe(TpivPP)(2-MeIm$^-$)]$^-$	2.11(2)	2.002(15)	0.52	0.65	2.045	NR[k]	NR[k]	5.1	14.7	42
average of the three values	2.114(4)	2.044(54)	0.55(2)	0.65(1)	2.042(5)					

[a]Estimated standard deviations are given in parentheses. [b]All complexes are high spin. [c]Averaged value. [d]Displacement of Fe from the mean plane of the four pyrrole N atoms. [e]Displacement of Fe from the 24-atom mean plane of the porphyrin core. [f]2-carbon, methyl-substituted. [g]Imidazole 4-carbon. [h]Off-axis tilt (deg) of the Fe−N$_{Im}$ bond from the normal to the porphyrin plane. [i]Dihedral angle between the plane defined by the closest N$_p$−Fe−N$_{Im}$ and the imidazole plane in deg. [j]Major imidazole orientation. [k]Not reported.

this derivative were 0.42 and 0.55 Å or a doming of 0.13 Å. Although this doming was initially thought to possibly be a general stereochemical feature of high-spin five-coordinate iron(II) derivatives, subsequent structure determinations of several related species showed that there was a wide variety of core conformations with an equally large variation in the (ΔN$_4$ − Δ) separation with values ranging from near zero to ∼0.15 Å.[19,25,38,39] Figures S5−S9 in the Supporting Information display the pair of mean plane diagrams for each of the derivatives in this study. The similar values for the hydrogen-bonded ethanol solvate and the tetramethylene sulfoxide solvate, both of which are at the upper limit of displacements, may be the result of the crystal packing influences as these two species pack isomorphously in similar crystallographic systems (see Table 1). The values of the two displacements for all hindered imidazole-ligated five-coordinate species are given in Table 3, along with several additional structural parameters.

The first two groups given in Table 3 are derivatives with an hydrogen-bonded imidazole and those without a hydrogen bond acceptor. Both groups show wide variation in doming, although the hydrogen-bonded group in the aggregate does show slightly larger iron displacements from both types of mean plane.

One possible effect of hydrogen bonding to the imidazole, which, in the limit, can be thought of as an imidazolate, is shown in Figure 3. The schematic on the left-hand side

DOI: 10.1021/acs.inorgchem.7b02744
Inorg. Chem. XXXX, XXX, XXX−XXX

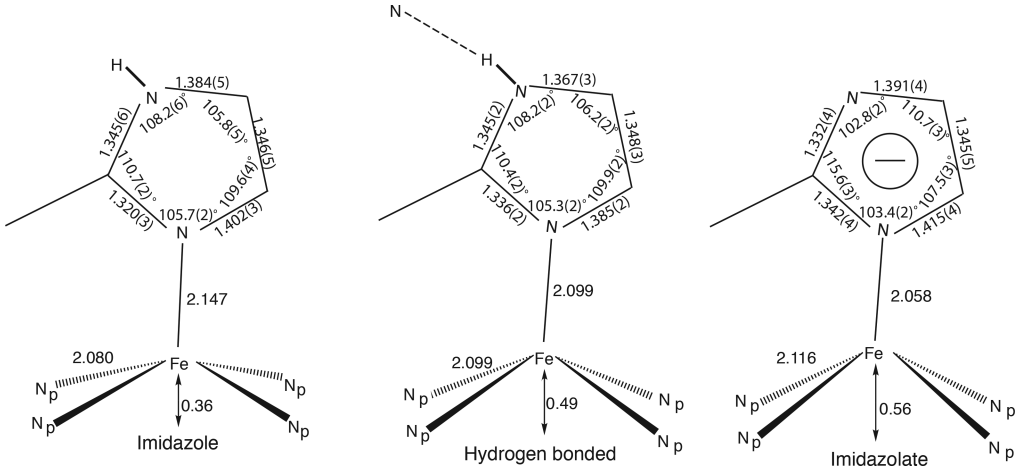

Figure 3. Schematic diagrams of the coordination group geometries found for a series of imidazole-ligated high-spin iron(II) porphyrinates with no hydrogen bond (left), an analogous species with a strong hydrogen bond to the coordinated imidazole (center), and imidazolate-ligated high-spin iron(II) porphyrinates (right). (Reprinted with permission from ref 25. Copyright 2008, American Chemical Society, Washington, DC.)

displays averaged values for several derivatives with no hydrogen bonding, whereas the schematic on the right-hand side shows averaged values from three derivatives, with imidazolate as the axial ligand. The data for the middle schematic comes from a single example with a hydrogen-bonded imidazole[23] that we will discuss later. Subsequent studies with other hydrogen-bond acceptors to the imidazole showed much smaller effects on the Fe atom displacements and values of the Fe−N_p and Fe−N_{im} bond distances, compared to the values displayed in the middle schematic of Figure 3. Values for other stereochemical parameters are also tabulated. There are an equal number of systems with no hydrogen bonding to the coordinated imidazole that are given in the second group of eight in Table 3. Averaged values for the selected parameters for each class are also given in the table. The estimated standard uncertainties following each averaged value were calculated based on the assumption that the values were drawn from the same population. The differences in the averaged values of the hydrogen-bonded derivatives, compared to those with no hydrogen bonds, are all toward those of imidazolate derivatives, although the differences are marginally significant, if at all.

Although the imidazole hydrogen atom was not located experimentally in any of the reported derivatives, the idealized position of the N−H hydrogen atom was used to calculate the N−H···A angle. The values calculated were 166° for the EtOH derivative, 170° for the TMSO derivative, and 166° for the two-site system. A neutron diffraction study located the hydrogen atom in the previous two-site system, where the N−H···N angle was found to be 163(2)°.[23]

The differences between most of the hydrogen-bonded derivatives and the example shown in Figure 3 (center) suggests the possibility that hydrogen bonding to coordinated imidazole can lead to a rather large range of effects on the coordination geometry and possibly on the electronic structure. The final derivative of this study provides additional evidence and understanding on this question. This final system is 2[Fe(TPP)(2-MeHIm)]·(2-MeHIm)·(C_6H_5Cl). This crystalline species has two distinct [Fe(TPP)(2-MeHIm)] sites: one with an imidazole solvate that hydrogen-bonds to the coordinated imidazole and a second center with no hydrogen bonding. This has been illustrated in Figure 2. There is a strong formal resemblance to an earlier study in which there were also two such [Fe(TPP)(2-MeHIm)] sites, but the first crystalline material did not have the chlorobenzene solvate.[23] The results of the distinct structures have been summarized in the third group of derivatives displayed in Table 3. The two Fe sites are labeled as Mol **1** and Mol **2**, with the current results also being denoted by prime symbols (Mol **1**′ and Mol **2**′). Although the hydrogen bond between the solvate imidazole and the coordinated imidazole are almost identical (the N···N distances are 2.824 Å for the first species and 2.843 Å for the new species), the coordination group geometries of Mol **2** and Mol **2**′ are very different. Mol **2** of the first system has coordination group parameters that are much different from either group 1 (hydrogen bonders) or group 2 (non-hydrogen bonders) and much closer to that of imidazolate (the last group of Table 3). However, the coordination group parameters of Mol **2**′ are similar to those of group 1. What are the reasons for the large differences between the two hydrogen-bonded species?

The additional solvate molecule (C_6H_5Cl) in the second system will certainly change the packing in the two crystalline solids. In principle, this allows a wide variety of differences in molecular conformations. We note two possibly significant differences, as a consequence of packing. The first is that there is a second hydrogen bond in the original two-site crystal system. The N−H group of the imidazole of Mol **1** forms a hydrogen bond to a porphyrin nitrogen of Mol **2** with a distance of 3.086 Å, thus leading to possible modest changes in electron density at the Fe site in Mol **2**. Generally, intermolecular interactions in the second crystal system do not appear substantially different, compared to the first system, but there is no additional hydrogen bond in the first system. The effect of this hydrogen bond must be to slightly increase the electron density of iron, relative to when the second hydrogen bond is not present.

A final important difference is found in the orientation of the hydrogen-bonded imidazole, with respect to directions in the porphyrin core. As has long been noted,[40] the dihedral angle between the imidazole plane and the closest Fe−N_P vector is typically small, nearly eclipsing this closest Fe−N_P bond. The observed values, usually called ϕ, are given for all imidazole derivatives in Table 3. As a group, the averaged value of ϕ for

DOI: 10.1021/acs.inorgchem.7b02744
Inorg. Chem. XXXX, XXX, XXX−XXX

the hydrogen-bonded species is 10.4°; both the average value and the range of values are smaller than those with no hydrogen bond. The observed value of ϕ for Mol **2′** is clearly much larger at 40.5°, outside the range of the commonly observed values, and also much larger than that seen for Mol **2**. This suggests that a *combination* of imidazole orientation and hydrogen-bonding influences are important in defining final coordination group parameters. Unfortunately, our sample for these possible effects is quite limited.

The steric bulk of the imidazole 2-methyl group leads to, in all derivatives examined to date, an off-axis tilt of the axial Fe−N_{Im} bond and a rotation of the imidazole ligand that leads to unequal Fe−N_{Im}−C_{Im} angles. The tilt angles range from 2.1° for [Fe(OEP)(2-MeHIm)]·(1,10-phen) (Mol **2**) to 11.4° for [Fe(TPP)(1,2-Me_2Im)]. This tilting is the partial result of minimizing the interaction between the bulky imidazole methyl group and the porphyrin core. Two important angles associated with the imidazole ligands (Fe−N_{Im}−C_{Im}) are given in Table 3. They range from 130.4(2)° to 133.7(2)° on the methyl side and from 121.2(2)° to 123.8(2)° on the other side. The off-axis tilt and imidazole rotation are correlated, to maximize the distance between the 2-methyl group and porphyrin core atoms; the values are similar across all imidazole-ligated species.

The Mössbauer data for the two distinct two-iron site systems clearly show that there are substantial differences between Mol **2** and Mol **2′** and smaller differences between Mol **1** and Mol **1′**. Both Fe systems were measured on selected single crystals labeled with 95% ^{57}Fe to ensure Mössbauer sample integrity. The original two-site system displayed two quadrupole doublets with distinct values of both the quadrupole splitting and isomer shift. The present two-site system shows an apparent single quadrupole doublet but with a somewhat unusual temperature-dependent line widths. This has been shown in Table 2. This is most consistent with a system displaying Mössbauer signals from two Fe centers with similar isomer shifts but with somewhat differing values of the quadrupole splitting. An attempt to disentangle the two signals using four overlapped Lorentzian lines, all with equal areas and equal line widths, is shown in Table 4. An example spectral fit

Table 4. Possible Partition of Mössbauer Parameters for 2[Fe(TPP)(2-MeHIm)]·(2-MeHIm)·(C_6H_5Cl)]

temperature, T (K)	ΔE_Q(mm/s)	δ_{Fe}(mm/s)
295	1.934, 1.708	0.796, 0.795
250	2.004, 1.742	0.829, 0.835
200	2.118, 1.855	0.862, 0.863
150	2.185, 1.920	0.883, 0.883
50	2.391, 2.116	0.894, 0.899
25	2.266	0.900

at 50 K is shown in Figure 4. Although the two quadrupole split doublets for 2[Fe(TPP)(2-MeHIm)]·(2-MeHIm)·(C_6H_5Cl)] do display differences, both the quadrupole splitting values and the isomer shift values are clearly in the range observed for imidazole-like species and not those of imidazolate-like species, as can be seen from the tabulation and comparisons given in Table 5. The Mössbauer data for this two-site system also show that the effects of hydrogen bonding are subtle and not easy to predict.

Both Fe sites in this new two-site system show a strong temperature dependence for the quadrupole splitting value.

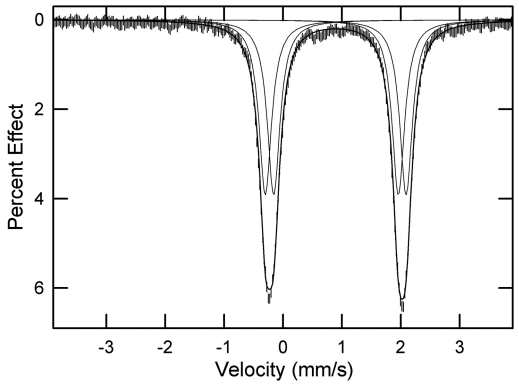

Figure 4. Experimental Mössbauer spectrum of 2[Fe(TPP)(2-MeHIm)]·(2-MeHIm)·(C_6H_5Cl) at 50 K. As described in the text, the spectrum is believed to be a pair of quadrupole split doublets. The diagram shows the fit made with the assumption that the areas and line widths of the doublets are equal.

ΔE_Q decreases strongly with increasing temperature. A similar pattern has been observed for other five-coordinate high-spin iron(II) porphyrinates with either tetraaryl or octaethyl peripheral substituents[19,38] and for deoxymyoglobin and deoxyhemoglobin.[41,49−54] The strong temperature dependence of ΔE_Q requires the presence of low-lying excited states above the quintet ground state.[52,55]

What is the best description of the electronic structure for imidazole-ligated high-spin iron(II) porphyrinates? Mössbauer studies by Lang and co-workers[41,49] first noted that the d-electron manifold (of the quintet state) must be very asymmetric, which requires that the d_{xz}- and d_{yz}-orbitals can no longer be degenerate. DFT calculations,[20] vetted by agreement with other physical properties, including the sign of ΔE_Q, lead to the following description. The doubly occupied d-orbital—the d_{xz}-orbital—is in a bonding combination with one component of the unoccupied $E_{(g)}$ LUMO of the porphyrin ring. This orbital is located in the plane of the coordinated imidazole. The next highest energy orbital is a hybrid of the singly occupied d_{yz}-orbital, in combination with the other component of the unoccupied $E_{(g)}$ LUMO of the porphyrin ring. This electronic state is distinctly different from that of high-spin derivatives with an anionic ligand where the doubly occupied orbital is the d_{xy}-orbital. This leads to large values of ΔE_Q (and opposite sign) and slightly larger values (~1.00 mm/s) for the isomer shift.

SUMMARY AND CONCLUSIONS

The synthesis and structures of four imidazole-ligated high-spin iron(II) porphyrinates have been reported. These were prepared as part of an effort to understand possible effects of hydrogen bonding to coordinated imidazole. Three of the four derivatives are found to have the desired hydrogen bond to imidazole. An analysis of the structural parameters shows that hydrogen bonding may have a small effect on geometry, relative to derivatives with no hydrogen bond. This follows the pattern now seen for hydrogen bonds versus no hydrogen bond. The electronic structure of one derivative has been examined by temperature-dependent Mössbauer spectroscopy. This derivative has two Fe sites: one with hydrogen bonding to the coordinated imidazole and one without hydrogen bonding to the coordinated imidazole. Only small differences were seen in the quadrupole splitting values, and no differences in the

DOI: 10.1021/acs.inorgchem.7b02744
Inorg. Chem. XXXX, XXX, XXX−XXX

Table 5. Solid-State Mössbauer Parameters for Five-Coordinate, High-Spin Imidazole-Ligated Iron(II) Porphyrinates and Related Species

complex	ΔE_Q (mm/s)	δ_{Fe} (mm/s)	η[a]	Γ[b]	temperature, T (K)	ref
[Fe(OEP)(2-MeHIm)]·(1,10-phen)	−1.93	0.94	0.76	0.43	4.2	25
[Fe(TPP)(2-MeHIm)]·(1,10-phen)	−2.12[c]	0.90		0.30	20	25
[Fe(TPP)(2-MeHIm)·(C_2H_5OH))	−2.28	0.93	0.8	0.31	4.2	41
[Fe(OEP)(1,2-Me_2Im)]	−2.19	0.92	0.50	0.37	4.2	19
[Fe(OEP)(2-MeHIm)]	−1.94	0.90	0.48	0.41	4.2	19
[Fe(T*p*-OCH_3PP)(1,2-Me_2Im)]	−2.44	0.95	0.68	0.46	4.2	38
[Fe(T*p*-OCH_3PP)(2-MeHIm)]	−2.18	0.94	0.58	0.58	4.2	38
[Fe(TPP)(1,2-Me_2Im)]	−1.93	0.92	0.53	0.44	4.2	38
[Fe(TTP)(2-MeHIm)]	−1.95	0.85	0.63	0.42	4.2	38
[Fe(TTP)(1,2-Me_2Im)]	−2.06	0.86	0.58	0.43	4.2	38
[Fe(TPP)(2-MeHIm)]	−2.40	0.92	0.8	0.50	4.2	39
[Fe(TPP)(1,2-Me_2Im)]	−2.16	0.92	0.7	0.25	4.2	41
[Fe((Piv_2C_8P)(1- MeIm)]	−2.3[c]	0.88	0.40	0.40	4.2	43
deoxyHb	−2.40	0.92	0.7	0.30	4.2	41
deoxyMb	−2.22	0.92	0.7	0.34	4.2	41
[Fe(TPP)(2-MeHIm)] (Mol **1′**)	> −2.27[c]	0.90				this work
[Fe(TPP)(2-MeHIm)]·(2-MeHIm) (Mol **2′**)	< −2.27[c]	0.90				this work
[Fe(TPP)(2-MeHIm)] (Mol **1**)	−2.40[d]	0.92	0.90	0.37	4.2	23
[Fe(TPP)(2-MeHIm)]·(2-MeHIm) (Mol **2**)	+2.94[d]	0.97	0.71	0.58	4.2	23
[K(222)][Fe(OEP)(2-$MeIm^-$)]	+3.71	1.00	0.22	0.31	4.2	18
[K(222)][Fe(TPP)(2-$MeIm^-$)]	+3.60	1.00	0.02	0.32	4.2	18
[Fe(TP_{piv}P)(2-MeIm)]$^-$	+3.51[e]	0.97			77	42
[Fe(TPP)(OC_6H_5)]$^-$	+4.01	1.03	0.25	0.38	4.2	44
[Fe)TP_{piv}P)(O_2CCH_3)]$^-$	+4.25	1.05	0.30	0.30	4.2	45
[Fe(TP_{piv}P)(OCH_3)]$^-$	+3.67[e]	1.03		0.40	4.2	46
[Fe(TP_{piv}P)(OC_6H_5)]$^-$	+3.90[e]	1.06		0.38	4.2	46
[$NaC_{12}H_{24}O_6$][Fe(TP_{piv}P)(SC_6HF_4)]	+2.38[e]	0.84		0.28	4.2	47
[Na(222)][Fe(T_{piv}PP)(SC_6HF_4)]	+2.38[e]	0.83		0.32	4.2	47
[Fe(T_{piv}PP)(SC_2H_5)]$^-$	+2.18	0.83	0.80	0.30	4.2	47
[Fe(T_{piv}PP)Cl]$^-$	+4.36[e]	1.01		0.31	77	48

[a]Asymmetry parameter. [b]Line width, fwhm. [c]Sign not determined experimentally, presumed negative. [d]Sign is based on a best fit. [e]Sign not determined experimentally, presumed positive.

isomer shifts were observed between the two independent Fe sites. None of the hydrogen-bonded systems of this study displayed properties near those of imidazolate systems, unlike the case in [Fe(TPP)(2-MeHIm)]$_2$·2-MeHIm.[23] We are left to conclude that there is a gradation of effects from hydrogen bonding, but with most displaying modest effects on geometry and electronic structure, relative to systems with no hydrogen bonding.

■ ASSOCIATED CONTENT

Supporting Information

The Supporting Information is available free of charge on the ACS Publications website at DOI: 10.1021/acs.inorgchem.7b02744.

ORTEP and mean plane drawings (Figures S1−S9); complete crystallographic details, coordinates, bond distances and angles, and thermal parameters (Tables S1−S24) (PDF)

Accession Codes

CCDC 1581485 (2[Fe(TPP)(2-MeHIm)]·(2-MeHim)·(C_6H_5Cl)), 1581486 ([Fe(TPP)(2-MeHIm)]·(TMSO)), 1581487 ([Fe(TPP)(2-MeHIm)]·(C_2H_5OH)), 1581488 ([Fe(TPP)(2-MeHIm)]·0.5(C_6H_5Cl)) contain the supplementary crystallographic data for this paper. These data can be obtained free of charge via www.ccdc.cam.ac.uk/data_request/cif, or by emailing data_request@ccdc.cam.ac.uk, or by contacting The Cambridge Crystallographic Data Centre, 12 Union Road, Cambridge CB2 1EZ, UK; fax: +44 1223 336033.

■ AUTHOR INFORMATION

Corresponding Authors

*E-mail: scheidt.1@nd.edu (W.R.S.).
*E-mail: cjhu@suda.edu.cn (C.H.).

ORCID

Chuanjiang Hu: 0000-0001-7126-3789
Bruce C. Noll: 0000-0003-3962-4358
W. Robert Scheidt: 0000-0002-6643-2995

Notes

The authors declare no competing financial interest.

■ ACKNOWLEDGMENTS

We thank the National Institutes of Health for support of this research, under Grant No. GM-38401. We thank the NSF for X-ray instrumentation support, through Grant No. CHE-0443233.

■ REFERENCES

(1) Cook, S. A.; Borovik, A. S. Molecular Designs for Controlling the Local Environments around Metal Ions. *Acc. Chem. Res.* **2015**, *48*, 2407−2414.

DOI: 10.1021/acs.inorgchem.7b02744
Inorg. Chem. XXXX, XXX, XXX−XXX

(2) Lehnert, N. Elucidating second coordination sphere effects in heme proteins using low-temperature magnetic circular dichroism spectroscopy. *J. Inorg. Biochem.* **2012**, *110*, 83−93.
(3) Valentine, J. S.; Sheridan, R. P.; Allen, L. C.; Kahn, P. Coupling between oxidation state and hydrogen bond conformation in heme proteins. *Proc. Natl. Acad. Sci. U. S. A.* **1979**, *76*, 1009−1013.
(4) Quinn, R.; Mercer-Smith, J.; Burstyn, J. N.; Valentine, J. S. Influence of hydrogen bonding on the properties of iron porphyrin imidazole complexes. An internally hydrogen bonded imidazole ligand. *J. Am. Chem. Soc.* **1984**, *106*, 4136−4144.
(5) Zarić, S. D.; Popović, D. M.; Knapp, E.-W. Factors Determining the Orientation of Axially Coordinated Imidazoles in Heme Proteins. *Biochemistry* **2001**, *40*, 7914−7928.
(6) Sahoo, D.; Quesne, M. G.; de Visser, S. P.; Rath, S. P. Hydrogen-Bonding Interactions Trigger a Spin-Flip in Iron(III) Porphyrin Complexes. *Angew. Chem., Int. Ed.* **2015**, *54*, 4796−4800.
(7) Salemme, F. R.; Freer, S. T.; Ng, H. X.; Alden, R. A.; Kraut, J. The Structure of Oxidized Cytochrome c_2 of *Rhodospirillum rubrum*. *J. Biol. Chem.* **1973**, *248*, 3910−3921.
(8) Peisach, J.; Blumberg, W. E.; Adler, A. Electron Paramagnetic Resonance Studies of Iron Porphyrin and Chlorin Systems. *Ann. N. Y. Acad. Sci.* **1973**, *206*, 310−327.
(9) Nicholls, P. The Role of The Protein In Haem Enzymes. *Biochim. Biophys. Acta* **1962**, *60*, 217−225.
(10) Mincey, T.; Traylor, T. G. Anion Complexes of Ferrous Porphyrins. *J. Am. Chem. Soc.* **1979**, *101*, 765−766.
(11) Teraoka, J.; Kitagawa, T. Resonance raman study of the heme-linked ionization in reduced horseradish peroxidase. *Biochem. Biophys. Res. Commun.* **1980**, *93*, 694−700.
(12) Morrison, M.; Schonbaum, G. R. Peroxidase-Catalyzed Halogenation. *Annu. Rev. Biochem.* **1976**, *45*, 861−888.
(13) Peisach, J. An Interim Report on Electronic Control of Oxygenation of Heme. *Ann. N. Y. Acad. Sci.* **1975**, *244*, 187−203.
(14) Poulos, T. L. Heme Enzyme Structure and Function. *Chem. Rev.* **2014**, *114*, 3919−3962.
(15) Jensen, K. P.; Ryde, U. Importance of proximal hydrogen bonds in haem proteins. *Mol. Phys.* **2003**, *101*, 2003−2018.
(16) Berglund, G. I.; Carlsson, G. H.; Smith, A. T.; Szöke, H.; Henriksen, A.; Hajdu, J. The catalytic pathway of horseradish peroxidase at high resolution. *Nature* **2002**, *417*, 463−468.
(17) Gajhede, M.; Schuller, D. J.; Henriksen, A.; Smith, A. T.; Poulos, T. L. Crystal structure of horseradish peroxidase C at 2.15 Å resolution. *Nat. Struct. Biol.* **1997**, *4*, 1032−1038.
(18) Hu, C.; Noll, B. C.; Schulz, C. E.; Scheidt, W. R. Proton-Mediated Electron Configuration Change in High-Spin Iron(II) Porphyrinates. *J. Am. Chem. Soc.* **2005**, *127*, 15018−15019.
(19) Hu, C.; An, J.; Noll, B. C.; Schulz, C. E.; Scheidt, W. R. Electronic Configuration of High-Spin Imidazole-Ligated Iron(II) Octaethylporphyrinates. *Inorg. Chem.* **2006**, *45*, 4177−4185.
(20) Hu, C.; Sulok, C. D.; Paulat, F.; Lehnert, N.; Twigg, A. I.; Hendrich, M. P.; Schulz, C. E.; Scheidt, W. R. Just a Proton: Distinguishing the Two Electronic States of Five-Coordinate High-Spin Iron(II) Porphyrinates with Imidazole/ate Coordination. *J. Am. Chem. Soc.* **2010**, *132*, 3737−3750.
(21) Collman, J. P.; Reed, C. A. Syntheses of Ferrous-Porphyrin Complexes. A Hypothetical Model for Deoxymyoglobin. *J. Am. Chem. Soc.* **1973**, *95*, 2048−2049.
(22) The following abbreviations are used in this paper OEP, dianion of octaethylporphyrin; TPP, dianion of *meso*-tetraphenylporphyrin; T*p*-OCH_3PP, dianion of *meso*-tetra-*p*-methoxyphenylporphyrin; TTP, dianion of *meso*-tetratolylporphyrin, TpivPP, dianion of *α,α,α,α*-tetrakis(*o*-pivalamidophenyl)porphyrin; Piv_2C_8P, dianion of *α,α*,15-[2,2′-(octanediamido)diphenyl]-*α,α*,10−20-bis(*o*-pivalamidophenyl)porphyrin; 2-MeHIm, 2-methylimidazole; 2-MeIm$^-$, 2-methylimidazolate; 1,2-Me_2Im, 1,2-dimethylimidazole; TMSO, tetramethylene sulfoxide; 222, 4,7,13,16,21,24-hexaoxo-1,10-diazabicyclo[8.8.8]hexacosane; N_P, porphyrinato nitrogen; Ct, the center of four porphyrinato nitrogen atoms.
(23) Hu, C.; Noll, B. C.; Piccoli, P. M. B.; Schultz, A. J.; Schulz, C. E.; Scheidt, W. R. Hydrogen Bonding Effects on the Electronic Configuration of Five-Coordinate High-Spin Iron(II) Porphyrinates. *J. Am. Chem. Soc.* **2008**, *130*, 3127−3136.
(24) Hu, C.; Scheidt, W. R. Unpublished observations.
(25) Hu, C.; Noll, B. C.; Schulz, C. E.; Scheidt, W. R. Hydrogen Bonding Influence of 1,10-Phenanthroline on Five-Coordinate High-Spin Imidazole-Ligated Iron(II) Porphyrinates. *Inorg. Chem.* **2008**, *47*, 8884−8895.
(26) Balch, A. L.; Watkins, J. J.; Doonan, D. J. Hydrogen bonding to coordinated imidazole. Association of 1,10-phenanthroline and other bases with bis(imidazole)metalloporphyrins. *Inorg. Chem.* **1979**, *18*, 1228−1231.
(27) The increase in imidazole binding constants upon the addition of 1,10-phenanthroline had been noted previously by Abbott and Rafson, but the origin of the effect has not been established. See: Abbott, E. H.; Rafson, P. A. Enhancement of ligand binding by iron(III) deuteroporphyrin(IX) dimethyl ester via interaction with 1,10-phenanthroline at a site remote from the metal ion. *J. Am. Chem. Soc.* **1974**, *96*, 7378−7379.
(28) Adler, A. D.; Longo, F. R.; Finarelli, J. D.; Goldmacher, J.; Assour, J.; Korsakoff, L. A simplified synthesis for meso-tetraphenylporphine. *J. Org. Chem.* **1967**, *32*, 476.
(29) (a) Adler, A. D.; Longo, F. R.; Kampas, F.; Kim, J. On the preparation of metalloporphyrins. *J. Inorg. Nucl. Chem.* **1970**, *32*, 2443−2445. (b) Buchler, J. W. Static Coordination Chemistry of Metalloporphyrins. In *Porphyrins and Metalloporphyrins*; Smith, K. M., Ed.; Elsevier Scientific Publishing: Amsterdam, The Netherlands, 1975; Chapter 5.
(30) (a) Fleischer, E. B.; Srivastava, T. S. The Structure and Properties of *μ*-Oxo-bis(tetraphenylporphineiron(III)). *J. Am. Chem. Soc.* **1969**, *91*, 2403−2405. (b) Hoffman, A. B.; Collins, D. M.; Day, V. W.; Fleischer, E. B.; Srivastava, T. S.; Hoard, J. L. The Crystal Structure and Molecular Stereochemistry of *μ*-Oxo-bis[*α,β,γ,δ*-tetraphenylporphinatoiron(III)]. *J. Am. Chem. Soc.* **1972**, *94*, 3620−3626.
(31) Landergren, M.; Baltzer, L. Convenient small-scale method for the insertion of iron into porphyrins. *Inorg. Chem.* **1990**, *29*, 556−557.
(32) Sheldrick, G. M. A short history of SHELX. *Acta Crystallogr., Sect. A: Found. Crystallogr.* **2008**, *A64*, 112−122.
(33) $R_1 = \sum||F_o| - |F_c||/\sum|F_o|$, $wR_2 = \{\sum[w(F_o^2 - F_c^2)^2]/\sum[w(F_o^2)^2]\}^{1/2}$ and $R(F^2) = \sum||F_o|^2 - |F_c|^2|/\sum|F_o|^2$. The conventional *R*-factors R_1 are based on *F*, with *F* set to zero for negative F^2. The criterion of $F^2 > 2\rho(F^2)$ was used only for calculating R_1. *R*-factors based on F^2 (wR_2) are statistically about twice as large as those based on *F*, and *R*-factors based on ALL data will be even larger.
(34) Sheldrick, G. M. *SADABS*; Universität Göttingen: Göttingen, Germany, 2006.
(35) Hu, C.; Schulz, C. E.; Scheidt, W. R. All High-Spin ($S = 2$) Iron(II) Hemes are NOT Alike. *Dalton Trans.* **2015**, *44*, 18301−18310.
(36) (a) Collman, J. P.; Kim, N.; Hoard, J. L.; Lang, G.; Radonovich, L. J.; Reed, C. A. Abstracts of Papers. In the *167th National Meeting of the American Chemical Society*, Los Angeles, CA, April 1974; American Chemical Society: Washington, DC, 1974; Paper No. INOR 29.
(37) Hoard, J. L. Personal communication to W.R.S. In particular, Prof. Hoard provided a complete set of atomic coordinates for the molecule.
(38) Hu, C.; Roth, A.; Ellison, M. K.; An, J.; Ellis, C. M.; Schulz, C. E.; Scheidt, W. R. Electronic Configuration Assignment and the Importance of Low-Lying Excited States in High-Spin Imidazole-Ligated Iron(II) Porphyrinates. *J. Am. Chem. Soc.* **2005**, *127*, 5675−5688.
(39) Ellison, M. K.; Schulz, C. E.; Scheidt, W. R. Structure of the Deoxymyoglobin Model [Fe(TPP)(2-MeHIm)] Reveals Unusual Porphyrin Core Distortions. *Inorg. Chem.* **2002**, *41*, 2173−2181.
(40) Scheidt, W. R.; Chipman, D. M. Preferred Orientation of Imidazole Ligands in Metalloporphyrins. *J. Am. Chem. Soc.* **1986**, *108*, 1163−1167.

DOI: 10.1021/acs.inorgchem.7b02744
Inorg. Chem. XXXX, XXX, XXX−XXX

(41) Kent, T. A.; Spartalian, K.; Lang, G.; Yonetani, T.; Reed, C. A.; Collman, J. P. High Magnetic Field Mössbauer Studies of Deoxymyoglobin, Deoxyhemoglobin, and Synthetic Analogues. *Biochim. Biophys. Acta, Protein Struct.* **1979**, *580*, 245−258.
(42) Mandon, D.; Ott-Woelfel, F.; Fischer, J.; Weiss, R.; Bill, E.; Trautwein, A. X. Structure and spectroscopic properties of five-coordinate (2-methylimidazolato)- and six-coordinate (imidazol-(imidazolato)iron(II) "picket-fence" porphyrins. *Inorg. Chem.* **1990**, *29*, 2442−2447.
(43) Momenteau, M.; Scheidt, W. R.; Eigenbrot, C. W.; Reed, C. A. A Deoxymyoglobin Model with a Sterically Unhindered Axial Imidazole. *J. Am. Chem. Soc.* **1988**, *110*, 1207−1215.
(44) Shaevitz, B. A.; Lang, G.; Reed, C. A. Susceptibility and Mössbauer Analysis of a High-Spin Ferrous Synthetic Heme with Unusually Large Quadrupole Splitting. *Inorg. Chem.* **1988**, *27*, 4607−4613.
(45) Bominaar, E. L.; Ding, X.; Gismelseed, A.; Bill, E.; Winkler, H.; Trautwein, A. X.; Nasri, H.; Fischer, J.; Weiss, R. Structural, Mössbauer, and EPR Investigations on Two Oxidation States of a Five-Coordinate, High-Spin Synthetic Heme. Quantitative Interpretation of Zero-Field Parameters and Large Quadrupole Splitting. *Inorg. Chem.* **1992**, *31*, 1845−1854.
(46) Nasri, H.; Fischer, J.; Weiss, R.; Bill, E.; Trautwein, A. X. Synthesis and Characterization of Five-Coordinate High-Spin Iron-(I1) Porphyrin Complexes with Unusually Large Quadrupole Splittings. Models for the P460 Center of Hydroxylamine Oxidoreductase from *Nitrosomonas*. *J. Am. Chem. Soc.* **1987**, *109*, 2549−2550.
(47) Schappacher, M.; Ricard, L.; Fischer, J.; Weiss, R.; Montiel-Montoya, R.; Bill, E.; Trautwein, A. X. Synthesis, Structure, and Spectroscopic Properties of Five-Coordinate Mercaptoiron(I1) Porphyrins. Models for the Reduced State of Cytochrome P450. *Inorg. Chem.* **1989**, *28*, 4639−4645.
(48) Schappacher, M.; Ricard, L.; Weiss, R.; Montiel-Montoya, R.; Gonser, U.; Bill, E.; Trautwein, A. X. Synthesis and Spectroscopic Properties of a Five-Coordinate Tetrafluorophenylthiolato Iron(II) icket FencePorphyrin Complex and its Carbonyl and Dioxygen Adducts: Synthetic Analogs for the Active Site of Cytochromes P450. *Inorg. Chim. Acta* **1983**, *78*, L9−L12.
(49) Kent, T. A.; Spartalian, K.; Lang, G. High magnetic field Mössbauer studies of deoxymyoglobin, deoxyhemoglobin, and synthetic analogues: Theoretical interpretations. *J. Chem. Phys.* **1979**, *71*, 4899−4908.
(50) Kent, T. A.; Spartalian, K.; Lang, G.; Yonetani, T. Mössbauer investigation of deoxymyoglobin in a high magnetic field. Orientation of the electric field gradient and magnetic tensors. *Biochim. Biophys. Acta, Protein Struct.* **1977**, *490*, 331−340.
(51) Eicher, H.; Bade, D.; Parak, F. Theoretical determination of the electronic structure and the spatial arrangement of ferrous iron in deoxygenated sperm whale myoglobin and human hemoglobin from Mössbauer experiments. *J. Chem. Phys.* **1976**, *64*, 1446.
(52) Huynh, B. H.; Papaefthymiou, G. C.; Yen, C. S.; Groves, J. L.; Wu, C. S. Electronic structure of Fe^{2+} in normal human hemoglobin and its isolated subunits. *J. Chem. Phys.* **1974**, *61*, 3750−3758.
(53) Eicher, H.; Trautwein, A. Electronic Structure of Ferrous Iron in Hemoglobin Inferred from Mössbauer Measurements. *J. Chem. Phys.* **1970**, *52*, 932−934.
(54) Eicher, H.; Trautwein, A. Electronic Structure and Quadrupole Splittings of Ferrous Iron in Hemoglobin. *J. Chem. Phys.* **1969**, *50*, 2540−2551.
(55) Hori, H.; Yashiro, H.; Ninomiya, K.; Horitani, M.; Kida, T.; Hagiwara, M. Low-lying electronic states of the ferrous high-spin (S = 2) heme in deoxy-Mb and deoxy-Hb studied by highly-sensitive multi-frequency EPR. *J. Inorg. Biochem.* **2011**, *105*, 1596−1602.

DOI: 10.1021/acs.inorgchem.7b02744
Inorg. Chem. XXXX, XXX, XXX−XXX